

## A neutron powder diffraction study of the ferroelectric relaxor $\text{Pb}(\text{Fe}_{1/2}\text{Ta}_{1/2})\text{O}_3$

This article has been downloaded from IOPscience. Please scroll down to see the full text article.

2001 J. Phys.: Condens. Matter 13 25

(<http://iopscience.iop.org/0953-8984/13/1/303>)

View [the table of contents for this issue](#), or go to the [journal homepage](#) for more

Download details:

IP Address: 171.66.16.226

The article was downloaded on 16/05/2010 at 08:16

Please note that [terms and conditions apply](#).

# A neutron powder diffraction study of the ferroelectric relaxor $\text{Pb}(\text{Fe}_{1/2}\text{Ta}_{1/2})\text{O}_3$

S A Ivanov<sup>1</sup>, S Eriksson<sup>2</sup>, N W Thomas<sup>3</sup>, R Tellgren<sup>4</sup> and H Rundlof<sup>4</sup>

<sup>1</sup> Karpov' Institute of Physical Chemistry, Moscow, Russia

<sup>2</sup> Inorganic Chemistry, Chalmers University of Technology, Gothenburg, Sweden

<sup>3</sup> Watts Blake Bearne and Co. plc., Newton Abbot TQ12 4PS, UK

<sup>4</sup> Inorganic Chemistry, The Ångström Laboratory, Uppsala University, Uppsala, Sweden

Received 24 March 2000, in final form 25 October 2000

## Abstract

The complex perovskite lead iron niobate,  $\text{Pb}(\text{Fe}_{1/2}\text{Ta}_{1/2})\text{O}_3$  (PFT), has been studied by neutron powder diffraction. Following collection of diffraction data at 300 K and at 10 K, structural refinements have been carried out by means of the Rietveld method. A straightforward unit cell of symmetry  $R3m$  was obtained for the 300 K structure, with the same symmetry, and a similar unit cell also obtained at the low temperature. In both cases, the iron and titanium ions were found to be disordered over the perovskite B-sites. Furthermore, in order to obtain a good agreement with experiment at 10 K, it was necessary to assign non-zero magnetic moments to the iron ions, these being in a collinear, antiferromagnetic arrangement. This magnetic structure can be described with reference to doubled unit cell axes. The factors governing the observed structures of PFT are discussed by comparison with the related system of  $\text{Pb}(\text{Fe}_{1/2}\text{Nb}_{1/2})\text{O}_3$ .

## 1. Introduction

Lead relaxor perovskite ferroelectrics are of great importance both to fundamental solid state physics and to modern technology, owing to their unique dielectric and electromechanical properties [1, 2]. In this connection, an understanding of the microscopic origins of the large frequency dispersion in these materials, of general formula  $\text{Pb}(\text{B}'\text{B}'')\text{O}_3$ , would pave the way for the generation of whole new classes of relaxors [3]. Although the main physical properties of these materials are well known, a detailed characterization of their crystal structures and microstructures is still needed [4]. It has also long been considered that lead-containing perovskites of this kind have suitable structures for studying the stereochemical peculiarities of the  $\text{Pb}^{2+}$  ion, these being directly associated with its non-bonded electron pair [5].

Lead iron tantalate,  $\text{Pb}(\text{Fe}_{1/2}\text{Ta}_{1/2})\text{O}_3$  (PFT), is one of the well known relaxor compounds belonging to the family of lead-based complex perovskites. For typical relaxors the  $\text{B}'$  cations are larger than their  $\text{B}''$  counterparts. However, in the case of PFT, the situation is reversed, as the  $\text{Fe}^{3+}$  ion is slightly smaller than the  $\text{Ta}^{5+}$  cation. In all likelihood because

of this anomalous relationship between the two B-ion radii, there are different points of view concerning the ferroelectric properties of PFT. It was pointed out in [3, 6] that PFT exhibited diffuse phase transformation behaviour, as is the case for relaxor ferroelectrics. However, in [7] this compound was considered to have normal ferroelectric properties. It is also pertinent to remark that the dielectric Curie behaviour,  $T_C$ , of PFT has not been unambiguously established. The ferroelectric Curie temperature of PFT was found to be 243K [9], but results of pyroelectric, dielectric and x-ray studies presented in [10] and [11] show that  $T_C$  of this compound ranges from 330 to 370K, depending on the nature of the specimens tested, principally whether they are in single crystal or ceramic form. Spontaneous polarization of single crystals manifests itself at temperatures below 320 K.

Numerous structural studies have been carried out in order to investigate the symmetry of PFT at room and low temperatures [8, 11–17]. The symmetry of non-cubic phases of PFT is still a matter for discussion [15–17], and its crystal chemistry is much more complicated than originally anticipated. According to an earlier report [9], PFT has a cubic perovskite ( $Pm\bar{3}m$ ) structure at room temperature, with  $\text{Fe}^{3+}$  and  $\text{Ta}^{5+}$  statistically distributed over B sites. However it was found later that the ceramic samples used contained minor amounts of a pyrochlore phase [18]. Although cubic symmetry was also reported for PFT at room temperature [13], other workers took the view that symmetry was lower than cubic [10, 12, 19]. At temperatures below 243 K, a ferroelectric phase with rhombohedral or monoclinic symmetry has been proposed [9]. It has also been proposed that the iron ions in PFT give rise to an antiferromagnetically ordered magnetic structure below  $\sim 180$  K [11].

In the light of the above considerations, further structural investigations of PFT are appropriate. In particular, a consideration of similarities and differences between the structures of lead-based relaxors of varying chemical compositions, as revealed by neutron powder diffraction, may help to determine the factors responsible for diffuse phase transitions in these ferroelectric materials. PFT itself may also be regarded as a model system for studying the relationship between ferroic and magnetic properties.

## 2. Experimental

Because the properties of ceramic samples are sensitive to the firing conditions, especially to firing temperature [2], we decided to perform our measurements on single crystals. The main results concerning the dielectric and pyroelectric studies of PFT single crystals have been published in [10].

Single crystals of PFT in the form of black cubes of side up to 3 mm were grown by the procedure described elsewhere [11]. The correct cationic compositions of the prepared single crystals were confirmed by x-ray spectroscopy (with the ARL-7200 spectrometer). Because the crystals obtained were highly twinned, all diffraction measurements were carried out on samples obtained by crushing the single crystals. The purities of the powder samples derived from single crystals were checked from the powder x-ray diffraction patterns obtained with a URD-63 diffractometer using  $\text{Cu K}\alpha$  radiation. These indicated a simple cubic perovskite unit cell ( $a = 4.007(1)$  Å) without ordering of Fe and Ta ions on octahedral sites, although it was noted that the high-angle peaks were somewhat broadened.

Neutron powder diffraction (NPD) data were collected at the Swedish Research reactor R2 in Studsvik ( $\lambda = 1.470$  Å). Diffractograms were registered at different temperatures using a 5 g sample contained in a vanadium can. Corrections for absorption effects were subsequently carried out in the Rietveld refinements, utilizing the empirical value  $\mu R = 0.133 \text{ cm}^{-1}$ . The step-scan covered the  $2\theta$  range  $4\text{--}139.95^\circ$  with a step-length  $0.05^\circ$ . Each experiment lasted for 17 hours. Nuclear and magnetic refinements were performed by the Rietveld method

**Table 1.** Results of the Rietveld refinements for different models of Pb disorder.

$hkl$	$\delta\text{Pb}$	$B_j$ ( $\text{\AA}^2$ )	$R_p$	$R_{wp}$	$R_B$	$R_f$	$R_{EXP}$
No	—	3.26(8)	4.44	6.07	6.68	4.78	3.88
100	0.069(5)	0.85(8)	4.46	6.10	5.88	4.08	3.88
110	0.054(2)	0.52(4)	4.40	6.02	6.49	4.99	3.88
111	0.041(1)	0.92(4)	4.42	6.03	6.69	4.94	3.88

using FULLPROF software [20]. Diffraction peaks were described by a pseudo-Voigt profile function, with a Lorentzian contribution to the Gaussian peak shape refined. A peak asymmetry correction was made for angles below  $35^\circ 2\theta$ . Background intensities were described by a polynomial with six coefficients.

The ideal cubic perovskite structure (space group (s.g.)  $Pm\bar{3}m$ ), where all atoms are fixed at special positions, was taken as a starting model for the Rietveld refinements of the neutron powder diffraction data of PFT at 300 K. At lower temperatures, where appropriate, the magnetic part of the diffractogram was treated as an additional ‘phase’. Since Mössbauer spectroscopy has provided strong support for the existence of the iron ions in the trivalent state, i.e.  $\text{Fe}^{3+}$  [12], the magnetic structure was refined in space group  $P1$  as an independent phase for which only the  $\text{Fe}^{3+}$  cations were defined. Only magnetic scattering was taken into consideration, with reflections up to  $2\theta = 60^\circ$  considered in the refinement, since the magnetic form factor renders negligible magnetic intensities at higher angles. Several magnetic models were tried in the refinement, each employing one additional refinement parameter, corresponding to the magnitudes of the magnetic moments.

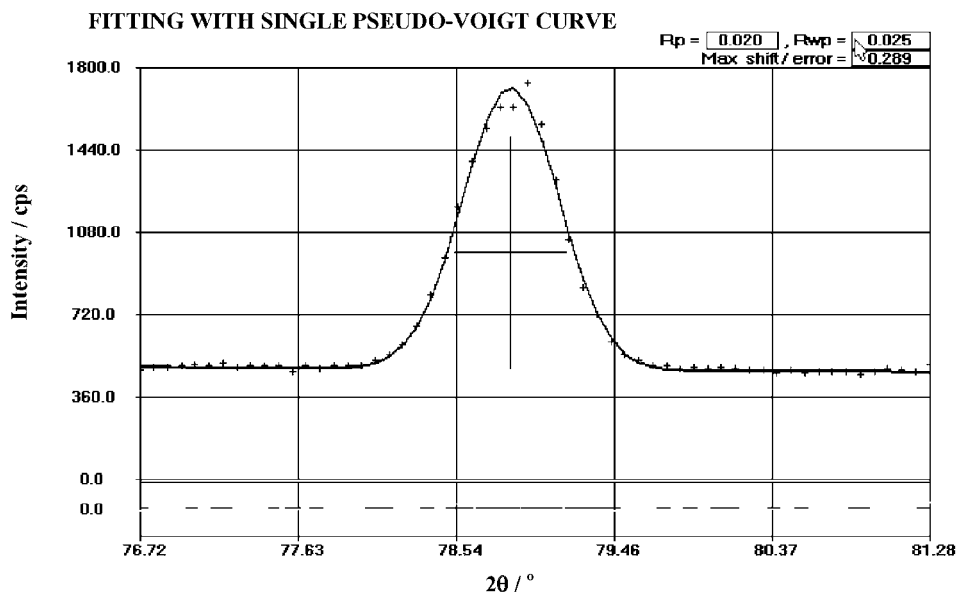
### 3. Results

Refinement of the room temperature structure in s.g.  $Pm\bar{3}m$  led to a very large temperature factor for the Pb cations,  $B_{Pb} = 3.39(8) \text{\AA}^2$ , in common with results obtained from other lead-containing perovskites [21–24]. A literal interpretation of this result, that the heaviest atoms in the PFT structure have the largest mean square displacements, is likely to be in error. It is more likely that the large  $B$ -values can be attributed some static or dynamic structural disorder. Indeed, structural disorder in the Pb sublattice is a common feature in lead-based perovskite oxides [3]. Pb is never found at its idealized special position, but rather statistically distributed over several sites around it.

In the next stage of our refinements, Pb was shifted from its high symmetry position successively along  $\langle 100 \rangle$ ,  $\langle 110 \rangle$  and  $\langle 111 \rangle$  directions. All three structural models refined successfully, leading to significant reductions in the thermal parameters of the Pb cations. The refined values of shifts, thermal parameters and  $R$ -factors are given in table 1. The best numerical improvement in the  $R_B$ -factor was obtained for the model in which the Pb cations statistically occupied the (6e) positions shifted along  $\langle 100 \rangle$  directions by a distance of  $0.28 \text{\AA}$ . However, the relevance of these results is open to question, owing to the strong correlation between the coordinates and the Debye–Waller factor.

A more accurate analysis of the neutron powder diffraction pattern of PFT using PROFIT software [25] indicated some additional features, which are incompatible with the cubic crystal system. Inspection of the room temperature neutron data showed that the broadening of high-angle reflections in the x-ray diffraction pattern was due to the presence of a small distortion away from cubic symmetry. Profile fitting of the (222) pseudocubic reflection, which shows a clearly recognizable shoulder (figures 1(a), (b)), led to a decomposition into two rhombohedral

(a)



(b)

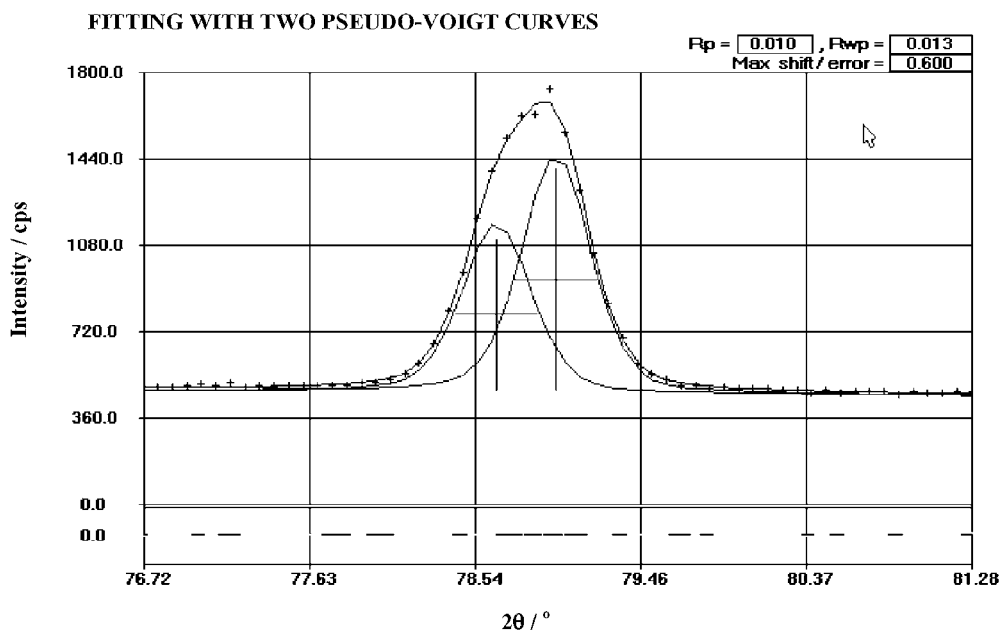


**Figure 1.** Profile fitting of the pseudo-cubic (222) reflection (a) by a single pseudo-Voigt curve; and (b) by two pseudo-Voigt curves (as would be necessary for rhombohedral symmetry). The improvement of the fitting with two profiles is quantified by the profile parameter  $R_p$ , which is equal to 0.020 for (a) and 0.010 for (b).

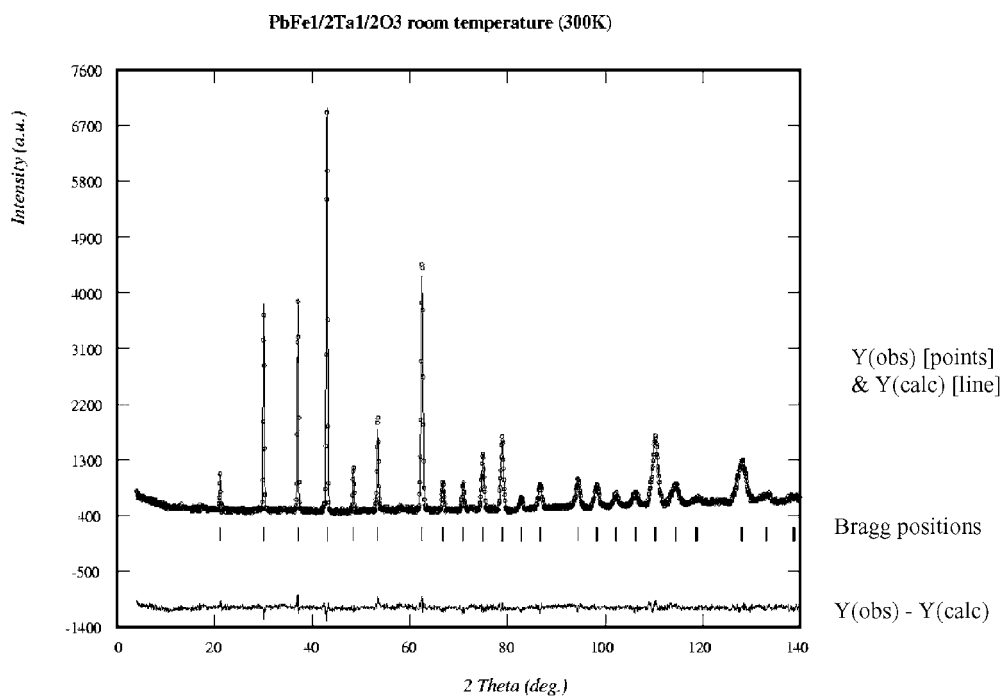


**Figure 2.** The neutron powder diffraction pattern obtained at 300 K, indicating the goodness of fit with the pattern calculated from the structural model in table 2.  $Y(\text{obs})$  refers to the observed diffraction pattern, and  $Y(\text{calc})$  to the calculated.

peaks,  $(222)R$  and  $(-222)R$ . Accordingly, the NPD pattern at 295K was subsequently refined in s.g.  $R3m$  (hexagonal description). Fe and Ta were assumed to occupy randomly the  $(3a)$  site in a 0.5:0.5 ratio. This variant gave the best fit to the collected data. Attempts to refine these data with tetragonal, orthorhombic and monoclinic structures resulted in either worse fits or negligibly small improvements of the  $R$ -factors. No extra peaks or additional splittings of main reflections were observed, which would indicate the need for a symmetry lower than rhombohedral. The final structural parameters for the rhombohedral structural solution are given in table 2, with the observed, calculated and difference profiles plotted in figure 2.

Refinement of the low temperature data (10 K) was also performed in the rhombohedral s.g.  $R3m$ . An examination of the NPD patterns of PFT obtained upon cooling into the antiferromagnetic region indicated the presence of magnetic peaks outside the Bragg positions given by the crystallographic unit cell (figure 3). The intensities of the additional peaks were found to fall to zero above the Néel temperature,  $T_N$ , giving strong support to the notion that they are magnetic in origin. Magnetic reflections were indexed with respect to a cell doubled in all three directions compared to the crystallographic unit cell, i.e.  $a = 2a_0 = 8.0096(8)$ ,  $\alpha = 89.93(1)$ . The optimum agreement with diffraction data (expressed by the minimum value of  $R_{\text{mag}}$ ) was obtained from an antiferromagnetic, G-type magnetic structure, with moments oriented parallel and anti-parallel to the trigonal axes (figure 4). Here every Fe cation is coupled antiferromagnetically to its six nearest neighbours. The refined value of the magnetic moment for the Fe cations at 10 K is  $3.08(4) \mu_B$ , which is much smaller than the expected value of effective magnetic moment per Fe ion of  $\mu_{\text{eff}} = 5.00 \mu_B$  ( $S = 5/2$ ). At the same time, this value is in reasonable agreement with the magnetic moments of Fe found previously in

**Table 2.** Crystal structure data for PFT at 10 and 300 K<sup>a</sup>.

	$T = 10 \text{ K}$	$T = 300 \text{ K}$
$a$ (Å)	5.6618(1)	5.6635(1)
$c$ (Å)	6.9407(2)	6.9444(2)
$B_{Pb}$ (Å <sup>2</sup> )	2.56(6)	3.17(7)
Fe/Ta ( $z$ )	0.483(1)	0.491(2)
$B_{Fe/Ta}$ (Å <sup>2</sup> )	0.13(5)	0.25(6)
O ( $x$ )	0.177(1)	0.171(2)
O ( $z$ )	0.342(2)	0.342(2)
$B_O$ (Å <sup>2</sup> )	0.99(7)	1.18(4)
Pb–O $\times 3$ (Å)	2.899(3)	2.904(5)
Pb–O $\times 6$ (Å)	2.833(3)	2.833(5)
Pb–O $\times 3$ (Å)	2.768(3)	2.764(5)
Fe/Ta–O $\times 3$ (Å)	2.001(3)	1.968(5)
Fe/Ta–O $\times 3$ (Å)	2.017(3)	2.046(5)
$R_P$	0.029	0.044
$R_{WP}$	0.037	0.059
$R_I$	0.045	0.053
$R_F$	0.032	0.041
$R_{EXP}$	0.040	0.039
$R_{MAG}$	0.054	

<sup>a</sup> In s.g.  $R\bar{3}m$ , the atoms have the following positions: Pb: 3m [0, 0, 0]; Fe/Ta: 3m [0, 0,  $z$ ]; O: 9b [ $x$ ,  $-x$ ,  $z$ ].

magnetically ordered Pb perovskites [26, 27]. The crystal structure of PFT corresponds to that of a B-site disordered perovskite, in which the Fe and Ta cations are distributed at random in the octahedral positions. Thus only 50% of these sites are occupied by the magnetic Fe<sup>3+</sup> ions. It is likely that the strengths of the antiferromagnetic interactions are severely reduced both by the disordered spatial distribution of the Fe ions and by the dilution caused by diamagnetic tantalum ions. Atomic coordinates and isotropic temperature factors of PFT at 10 K are listed in table 2.

For completeness, a monoclinic structure (s.g.  $Cm$ ) was also investigated for the low temperature phase of PFT, as proposed elsewhere [16, 17]. However, this model did not lead to significant improvements in the values of  $R$ -factors compared to those quoted for rhombohedral symmetry in table 2, even though the number of refinement variables had been increased.

**Table 3.** Crystal structure parameters of the proposed structures of PFT at 300 K and 10 K, utilizing the following parameters [28]:  $V_{Pb}$ : PbO<sub>12</sub> polyhedral volume;  $V_{Fe/Ta}$ : FeO<sub>6</sub>/TaO<sub>6</sub> polyhedral volume;  $\Delta s$ : octahedral distortion perpendicular to trigonal axis;  $\eta$ : octahedral elongation parallel to trigonal axis;  $\Delta z_{Pb}$ ,  $\Delta z_{Fe/Ta}$ : displacements of Pb and Fe/Ta ions parallel to trigonal axis.

$T$ (K)	$V_{Pb}$ (Å <sup>3</sup> )	$V_{Fe/Ta}$ (Å <sup>3</sup> )	$V_{Pb}/V_{Fe/Ta}$ (Å <sup>3</sup> )	$\Delta s$ (pm)	$\eta$	$\Delta z_{Pb}$ (pm)	$\Delta z_{Fe/Ta}$ (pm)
300	53.584	10.717	5	6.68	1.001 15	5.88	12.20
10	53.523	10.705	5	17.21	1.000 92	5.88	17.47

#### 4. Discussion

The above results indicate that our sample of PFT has a polar rhombohedral lattice at room temperature, rather than a cubic one. This conclusion is in agreement with the observation

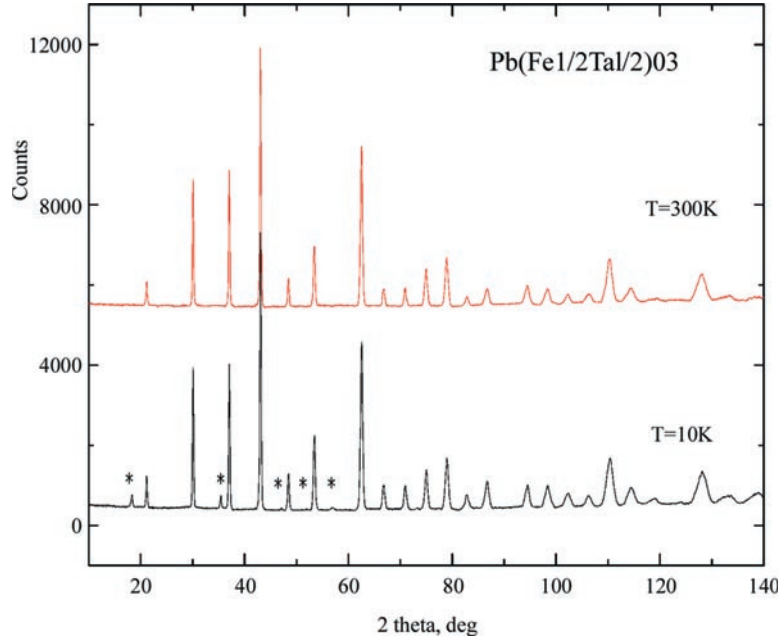


**Figure 3.** Comparison of the low temperature and room temperature neutron powder diffraction patterns, with magnetic reflections indicated by stars.

of spontaneous polarization at 320 K in [11] and results of complex physico-chemical investigations of the same crystals [10], which indicated that the Curie temperature of PFT ranges from 330 to 370 K. Although the deviation from the cubic symmetry of PFT is very small, accurate information about the true symmetry of relaxors is important for a full understanding of the mechanism of ferroelectricity.

In both the rhombohedral and the monoclinic refinements the displacement factor of Pb was found to be large, which suggests some positional disorder. Furthermore, a reduction in temperature leaves this disorder unaltered. This phenomenon is likely to be due to the electronic configuration of the  $\text{Pb}^{2+}$  cation. Whereas the highly directional nature of the bonding in Pb perovskites can be explained by the presence of the lone electron pair, the likely disorder of  $\text{Pb}^{2+}$  cation could also be due to repulsions between its lone electron pair and the Pb–O interactions formed with its coordination polyhedron. Such Pb displacements from high symmetry positions could increase the angles between the lone-electron pair and all Pb–O bonds, thereby minimizing these repulsion effects. However, additional experimental study is required here. In summary Pb disorder is present in both polar and non-polar phases of PFT.

Derived parameters describing  $\text{PbO}_{12}$  and  $\text{FeO}_6/\text{TaO}_6$  polyhedral volumes, along with octahedral distortions and ionic displacements along the polar axis are given in table 3. The volumes  $V(\text{Pb})$  and  $V(\text{Fe}/\text{Ta})$  decrease upon cooling. They are marginally smaller than those for  $\text{Pb}(\text{Fe}_{1/2}\text{Nb}_{1/2})\text{O}_3$  (PFN) [27], indicating a slightly smaller ionic radius of  $\text{Ta}^{5+}$  compared to  $\text{Nb}^{5+}$ . However, the  $\Delta z_{\text{Fe}/\text{Ta}}$  values at both 300 K and 10 K of PFT are virtually identical to the corresponding values of  $\Delta z_{\text{Fe}/\text{Nb}}$  in PFN at these temperatures. The lower  $T_c$  values of PFT therefore point towards the greater polarizability of the  $\text{Nb}^{5+}$  ions compared to  $\text{Ta}^{5+}$ . The increase in  $\Delta s$  in going from 300 K to 10 K in PFT can be correlated to the increase in  $\Delta z_{\text{Fe}/\text{Ta}}$ : the oxygen octahedron becomes more distorted in order to accommodate a larger B-ion displacement. Octahedral elongations  $\eta$  are similar at both 300 and 10 K in PFT,



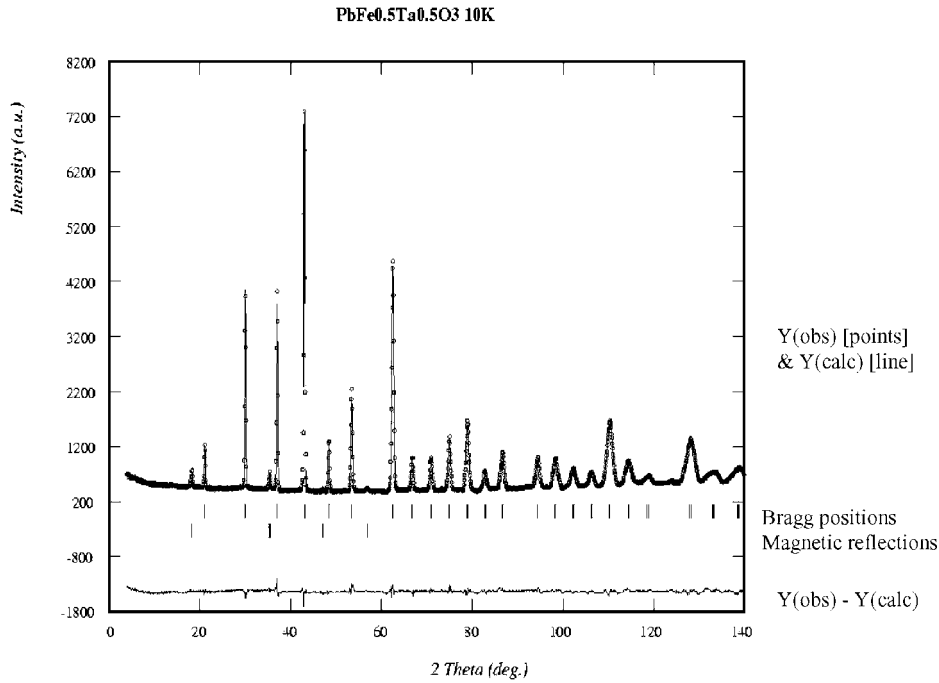


**Figure 4.** The neutron powder diffraction pattern obtained at 10 K, indicating the goodness of fit with the pattern calculated from the structural model in table 2.  $Y(\text{obs})$  and  $Y(\text{calc})$  have the same meanings as in figure 2, with the additional bars labelled 'magnetic reflections' signifying non-Bragg reflections.

unlike the case for PFN, where  $\eta$  increases markedly between 300 and 10 K. The  $\Delta_{zpb}$  does not change between 300 and 10 K for PFT, unlike the case for PFN, where this parameter increases significantly between 300 and 10 K.

It is to be noted that the results of our work are at variance with the findings of Lampis *et al* [29]. These authors have proposed that PFT exists in a cubic phase for temperatures greater than 270 K, whereas we propose rhombohedral symmetry. Furthermore, they propose a small tetragonal distortion at 230 K and *monoclinic* symmetry at low temperatures, based on data collected at 130 and 15 K. The view that monoclinic symmetry is found at low temperatures is also in disagreement with our proposed rhombohedral solution. It will be recalled that monoclinic symmetry has been explored in our work, as a possibility for the low temperature structure. However, this option did not lead to any significant improvement in the fitting. It is also pertinent to remark that Lampis *et al* did not consider the magnetic scattering of neutrons in their work. Thus, in order to rationalize the appearance of additional peaks at low temperature, they will have been forced to postulate a symmetry lower than rhombohedral. So we propose the existence of rhombohedral symmetry, both at 300 and at 10 K, with the extra peaks observed at low temperature due to magnetic ordering.

A remaining, unsolved problem concerns the differences in dielectric properties of  $\text{Pb}(\text{Fe}_{0.5}\text{Nb}_{0.5})\text{O}_3$  and  $\text{Pb}(\text{Fe}_{0.5}\text{Ta}_{0.5})\text{O}_3$  ceramics. Even though both systems have similar, disordered rhombohedral structures, PFT shows typical relaxor behaviour, whereas PFN exhibits only a small degree of frequency dispersion. Since the two parameters of charge and radius are similar for both  $\text{Ta}^{5+}$  and  $\text{Nb}^{5+}$  ions, the implication is that a full atomistic understanding of these differences will rest on a consideration of different electronic structures,

as might be expressed by differing electronic polarizabilities or, alternatively, degrees of covalency. A resolution of this problem is reserved for future work.

### Acknowledgments

The authors thank the Royal Swedish Academy of Sciences for financial support of this research.

### References

- [1] Cross L E 1987 *Ferroelectrics* **76** 241  
Cross L E 1994 *Ferroelectrics* **151** 305
- [2] Yokosuka M 1995 *Japan. J. Appl. Phys.* **43** 214
- [3] Ye Z G 1998 *Key Eng. Materials* **155–156** 81
- [4] Venetsev Yu N, Politova E D and Ivanov S A 1985 *Ferro- and Antiferroelectrics of Barium Titanate Family* (Moscow: Chemistry)
- [5] Alonso J A and Rasines I 1988 *J. Phys. Chem. Solids* **49** 385
- [6] Fujimoto S, Yasuda N, Teresawa H and Kato Y 1986 *Proc. 6th IEEE Int. Symp. on Applied Ferroelectrics* (Bethlehem, USA) p 107
- [7] Lee B H, Kim N K, Kim J J and Cho S H 1998 *J. Korean Phys. Soc.* **32** 978
- [8] Randall C A, Bhacla A S, Shrout T R and Cross L E 1990 *J. Mater. Res.* **5** 829
- [9] Smolenskii G A, Agranovskaia A I and Isupov V A 1959 *Fiz. Tverd. Tela* **1** 990
- [10] Venetsev Yu N, Skorohodov N E and Chechkin V V 1992 *Ferroelectrics* **137** 57
- [11] Nomura S, Takabayashi H and Nakagawa T 1968 *Japan. J. Appl. Phys.* **7** 600
- [12] Nomura S, Kaneta K and Abe M 1979 *Japan. J. Appl. Phys.* **18** 681
- [13] Brixel W, Rivera J P and Schmid H 1984 *Ferroelectrics* **55** 181
- [14] Ivanov S A, Ter-Mikaelyan G B and Venetsev Yu N 1984 *Ferroelectrics* **56** 1029
- [15] Lehmann A G, Kubel F, Ye Z G and Schmid H 1995 *Ferroelectrics* **172** 277
- [16] Lehmann A G, Kubel F and Schmid H 1997 *J. Phys.: Condens. Matter* **9** 8201
- [17] Lehmann A G and Sciau P 1999 *J. Phys.: Condens. Matter* **11** 1235
- [18] Agranovskaya A I 1960 *Izv. Akad. Nauk SSSR Ser. Fiz.* **24** 1275
- [19] Kochetkov V V and Venetsev Yu N 1979 *Izv. Akad. Nauk SSSR Neorg. Mater.* **15** 1833
- [20] Rodrigues-Carvajal J 1993 *Physica B* **192** 55
- [21] Knight K S and Baba-Kishi K Z 1995 *Ferroelectrics* **173** 341
- [22] Lampis N, Sciau P and Lehmann A G 1999 *J. Phys.: Condens. Matter* **11** 3489
- [23] Malibert C, Dkhil B, Kiat J M, Durand D, Berar J F and Spasojevic-de-Bire A 1997 *J. Phys.: Condens. Matter* **9** 7485
- [24] Thomas N W, Ivanov S A, Ananta S, Tellgren R and Rundlof H 1999 *J. Eur. Ceram. Soc.* **19** 2667
- [25] Zhurov V V and Ivanov S A 1996 *Kristallographia* **40** 156
- [26] Pietrzak J, Maryanowska A and Leciejewicz J 1981 *Phys. Status Solidi a* **65** K79
- [27] Ivanov S A, Tellgren R, Rundlof H, Thomas N W and Ananta S 2000 *J. Phys.: Condens. Matter* **12** 2393
- [28] Thomas N W and Beitollahi A 1994 *Acta Crystallogr. B* **50** 549
- [29] Lampis N, Sciau P and Lehmann A G 2000 *J. Phys.: Condens. Matter* **12** 2367